Chapter 8: Major Elements

Carbonaceous chondrites

Compositions from
Allende meteorite ⇒

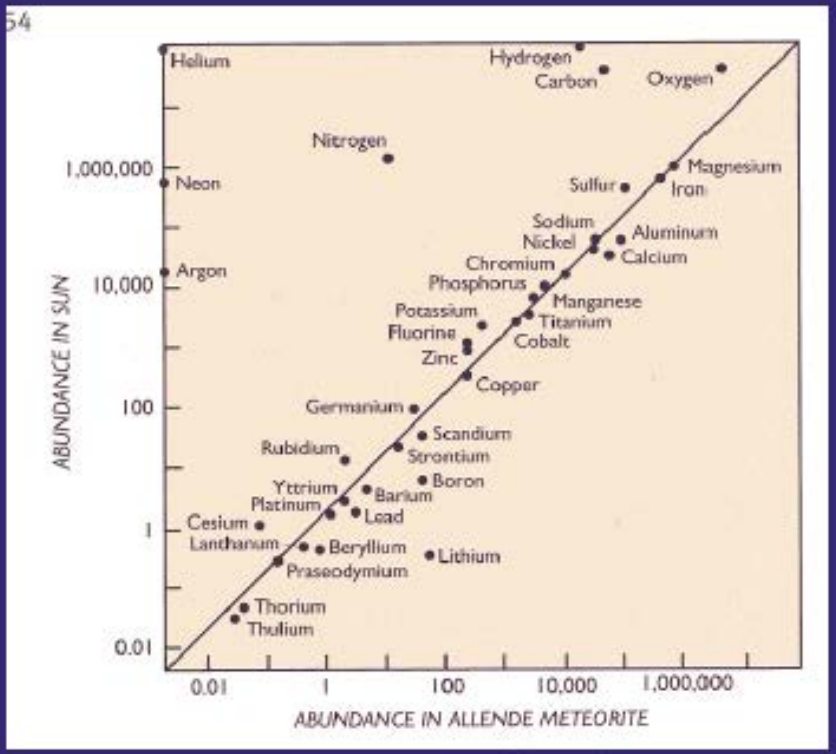

Ref.: J. K. Beatty et al., *The New Solar System*, Ch. 26

Carbonaceous chondrites are considered to be the most similar in composition to the solar nebula

Element	Wt % Oxide	Atom %
O		60.8
Si	59.3	21.2
Al	15.3	6.4
Fe	7.5	2.2
Ca	6.9	2.6
Mg	4.5	2.4
Na	2.8	1.9

Abundance of the elements in the Earth's crust

Major elements: usually greater than 1%

SiO_2 Al_2O_3 FeO* MgO CaO Na_2O K_2O H_2O

Minor elements: usually 0.1 - 1%

TiO_2 MnO P_2O_5 CO_2

Trace elements: usually < 0.1%

everything else

A typical rock analysis

Wt. % Oxides to Atom % Conversion				
Oxide	Wt. %	Mol Wt.	Atom prop	Atom %
SiO_2	49.20	60.09	0.82	12.25
TiO_2	1.84	95.90	0.02	0.29
Al_2O_3	15.74	101.96	0.31	4.62
Fe_2O_3	3.79	159.70	0.05	0.71
FeO	7.13	71.85	0.10	1.48
MnO	0.20	70.94	0.00	0.04
MgO	6.73	40.31	0.17	2.50
CaO	9.47	56.08	0.17	2.53
Na_2O	2.91	61.98	0.09	1.40
K_2O	1.10	94.20	0.02	0.35
H_2O^+	0.95	18.02	0.11	1.58
(O)			4.83	72.26
Total	99.06		6.69	100.00

Must multiply by # of cations in oxide ↑

Table 8-3. Chemical analyses of some representative igneous rocks

	Peridotite	Basalt	Andesite	Rhyolite	Phonolite
SiO_2	42.26	49.20	57.94	72.82	56.19
TiO_2	0.63	1.84	0.87	0.28	0.62
Al_2O_3	4.23	15.74	17.02	13.27	19.04
Fe_2O_3	3.61	3.79	3.27	1.48	2.79
FeO	6.58	7.13	4.04	1.11	2.03
MnO	0.41	0.20	0.14	0.06	0.17
MgO	31.24	6.73	3.33	0.39	1.07
CaO	5.05	9.47	6.79	1.14	2.72
Na_2O	0.49	2.91	3.48	3.55	7.79
K_2O	0.34	1.10	1.62	4.30	5.24
H_2O+	3.91	0.95	0.83	1.10	1.57
Total	98.75	99.06	99.3	99.50	99.23

CIPW Norm

- ***Mode*** is the volume % of minerals seen
- ***Norm*** is a calculated "idealized" mineralogy

	Fo	En	Q
SiO_2	42.7	59.9	100
MgO	57.3	40.1	

Variation Diagrams

How do we display chemical data in a meaningful way?

Bivariate (x-y) diagrams

Harker diagram for Crater Lake

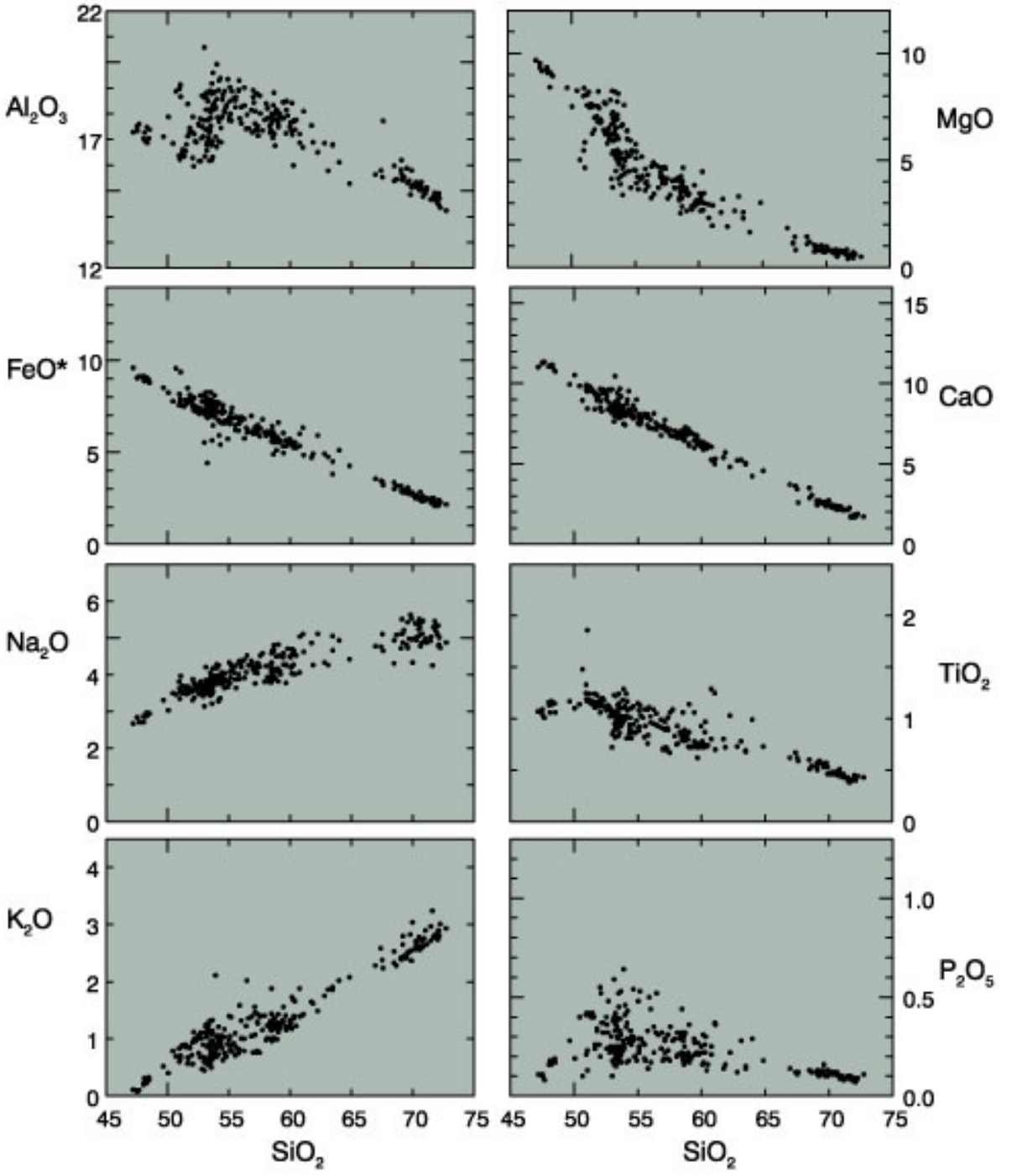

Figure 8.2. Harker variation diagram for 310 analyzed volcanic rocks from Crater Lake (Mt. Mazama), Oregon Cascades. Data compiled by Rick Conrey (personal communication).

Bivariate (x-y) diagrams

Harker diagram for Crater Lake

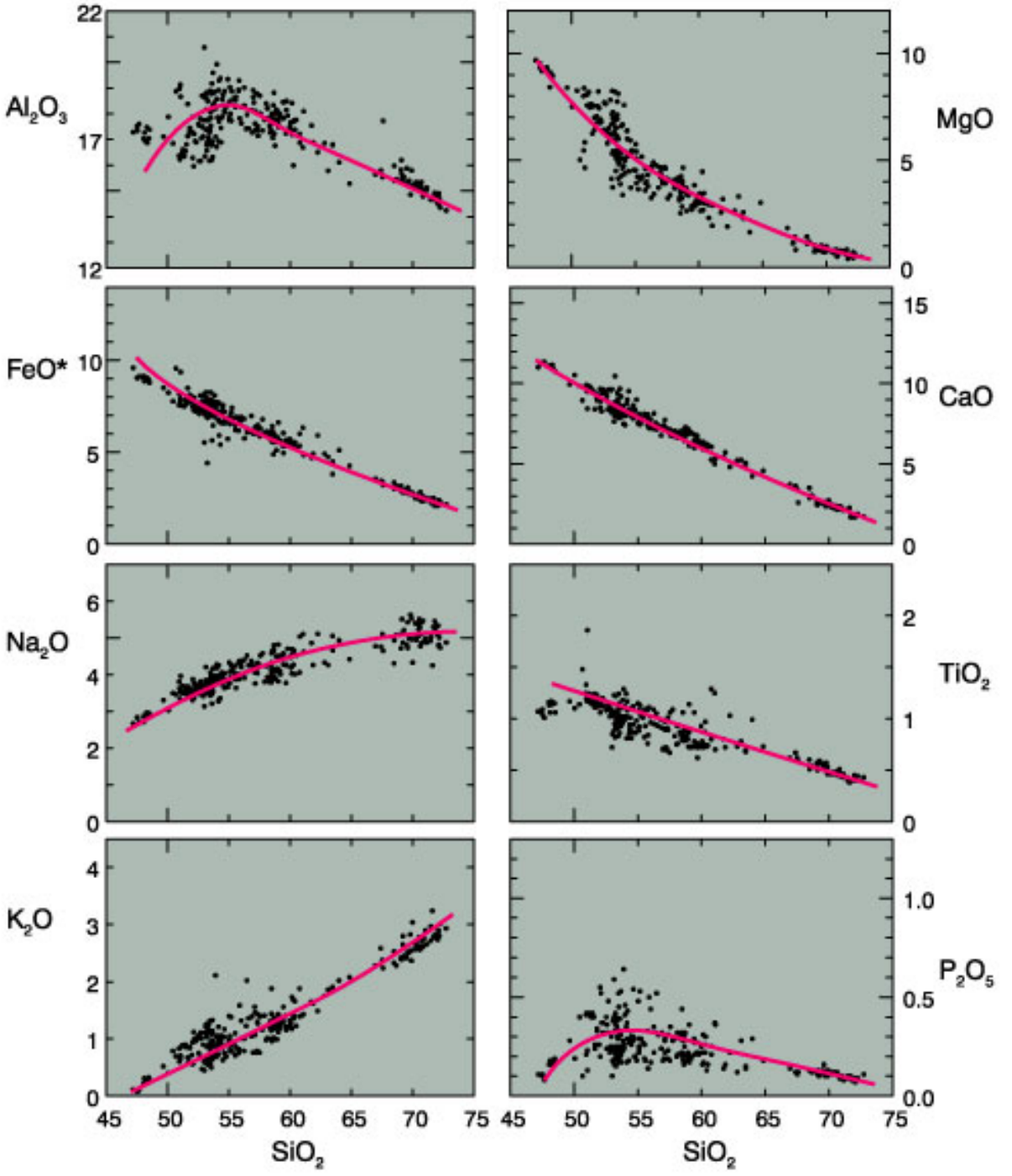

Figure 8.2. Harker variation diagram for 310 analyzed volcanic rocks from Crater Lake (Mt. Mazama), Oregon Cascades. Data compiled by Rick Conrey (personal communication).

Ternary Variation Diagrams

Example: AFM diagram

(alkalis-FeO*-MgO)

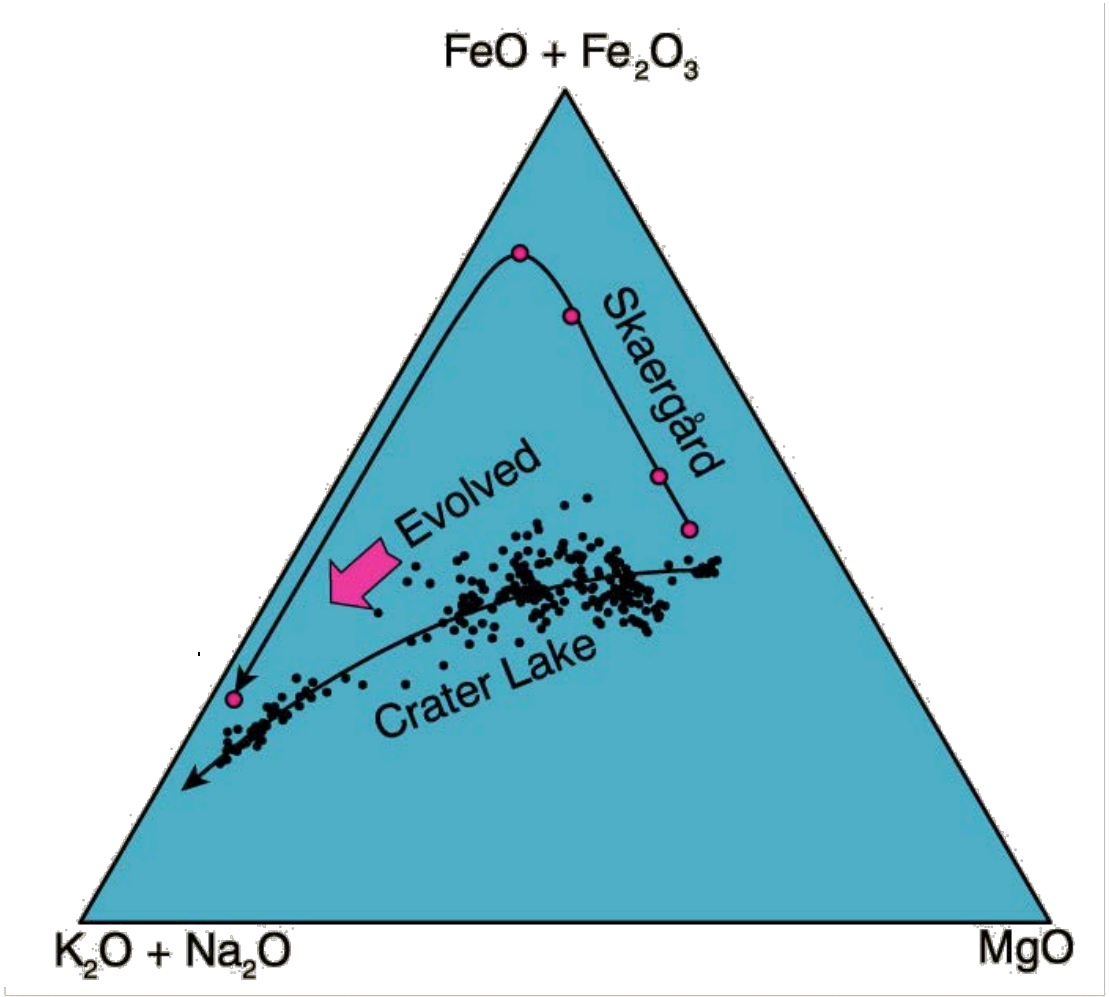

Figure 8.3. AFM diagram for Crater Lake volcanics, Oregon Cascades. Data compiled by Rick Conrey (personal communication).

Models of Magmatic Evolution

Table 8-5 . Chemical analyses (wt. %) of a hypothetical set of related volcanics.

Oxide	B	BA	A	D	RD	R
SiO_2	50.2	54.3	60.1	64.9	66.2	71.5
TiO_2	1.1	0.8	0.7	0.6	0.5	0.3
Al_2O_3	14.9	15.7	16.1	16.4	15.3	14.1
Fe_2O_3*	10.4	9.2	6.9	5.1	5.1	2.8
MgO	7.4	3.7	2.8	1.7	0.9	0.5
CaO	10.0	8.2	5.9	3.6	3.5	1.1
Na_2O	2.6	3.2	3.8	3.6	3.9	3.4
K_2O	1.0	2.1	2.5	2.5	3.1	4.1
LOI	1.9	2.0	1.8	1.6	1.2	1.4
Total	99.5	99.2	100.6	100.0	99.7	99.2

B = basalt, BA = basaltic andesite, A = andesite, D = dacite, RD = rhyo-dacite, R = rhyolite. Data from Ragland (1989)

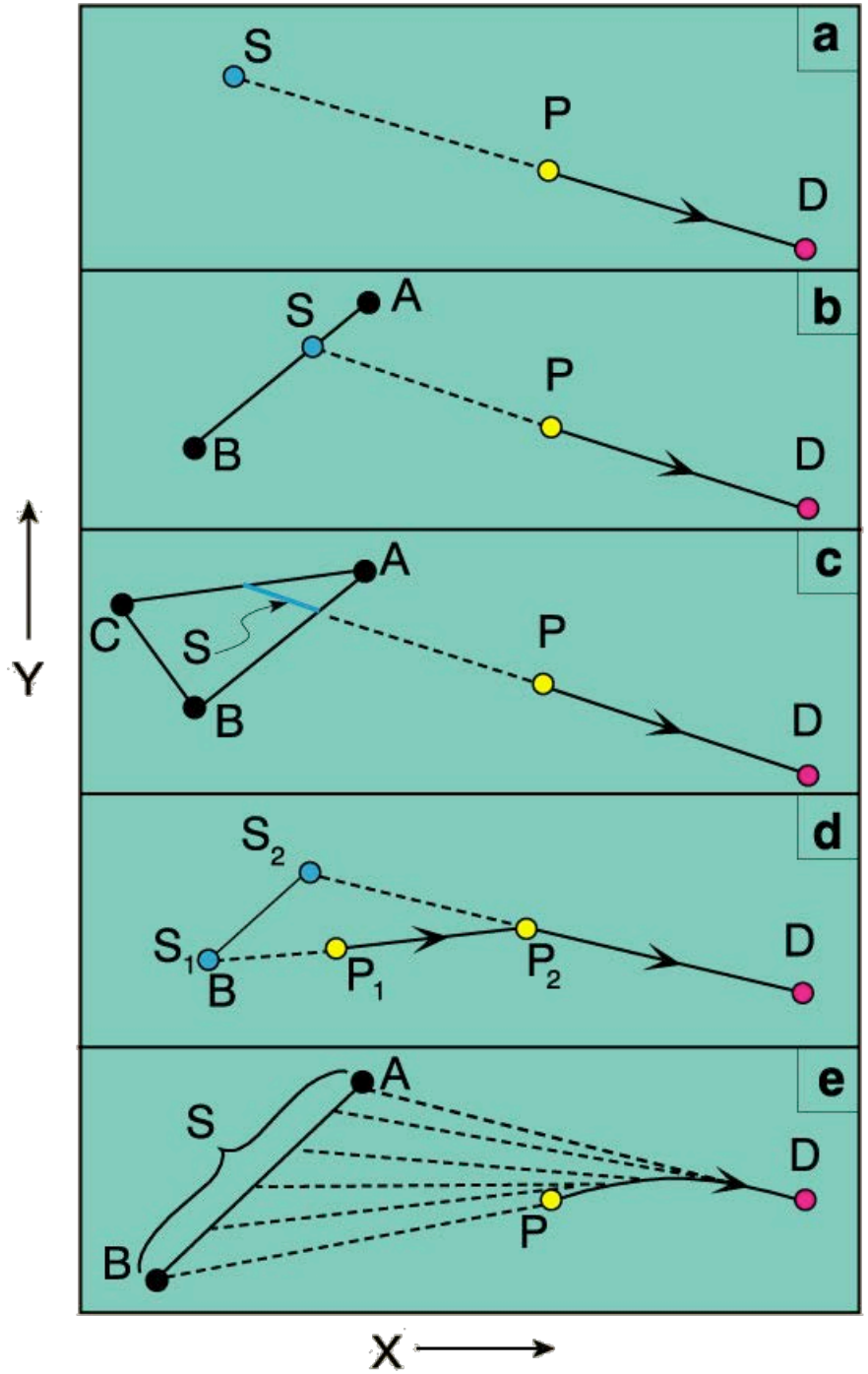

Figure 8.6. Stacked variation diagrams of hypothetical components X and Y (either weight or mol %). P = parent, D = daughter, S = solid extract, A, B, C = possible extracted solid phases. For explanation, see text. From Ragland (1989). Basic Analytical Petrology, Oxford

Harker diagram

- Smooth trends
- Model with 3 assumptions:

1 Rocks are related by FX

2 Trends = liquid line of descent

3 The basalt is the parent magma from which the others are derived

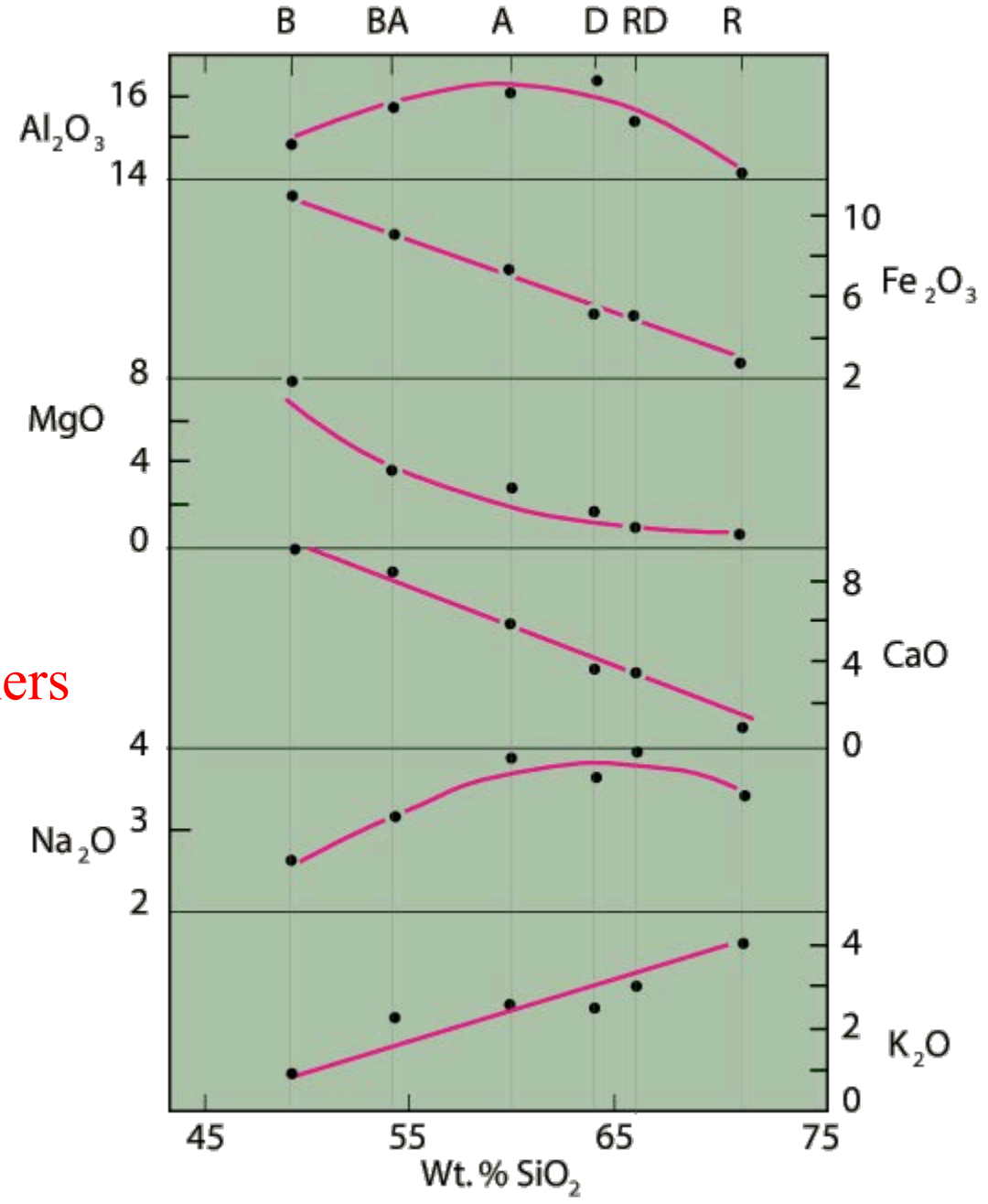

Figure 8.7. Stacked variation diagrams of hypothetical components X and Y (either weight or mol %). P = parent, D = daughter, S = solid extract, A, B, C = possible extracted solid phases. For explanation, see text. From Ragland (1989). Basic Analytical Petrology, Oxford

- Extrapolate BA → B and further to low SiO_2
- K_2O is first element to → 0 (at $SiO_2 = 46.5$)

46.5% SiO_2 is interpreted to be the concentration in the bulk solid extract and the blue line → the concentration of all other oxides

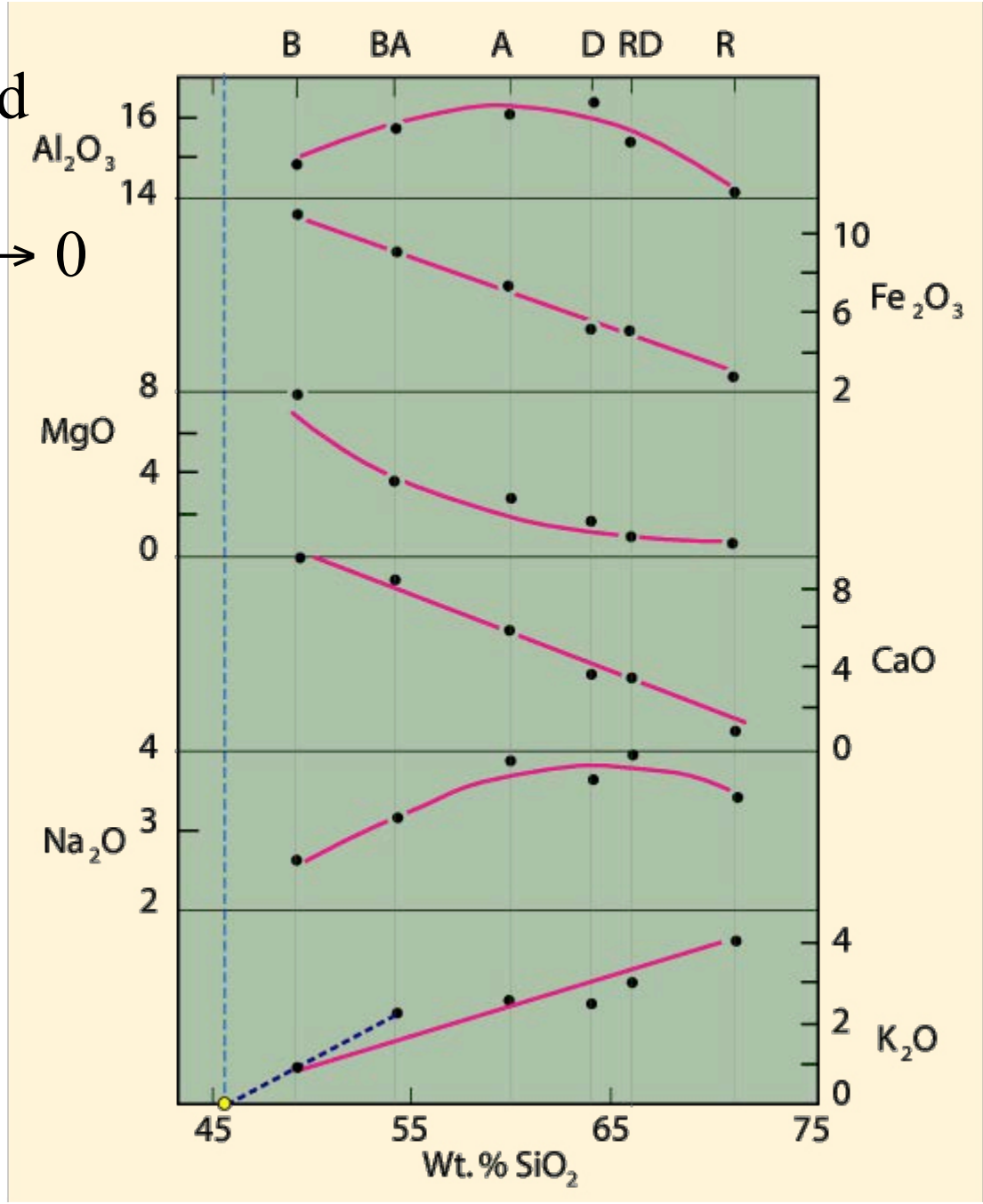

Figure 8.7. Stacked variation diagrams of hypothetical components X and Y (either weight or mol %). P = parent, D = daughter, S = solid extract, A, B, C = possible extracted solid phases. For explanation, see text. From Ragland (1989). Basic Analytical Petrology, Oxford

Extrapolate the other curves back BA → B → blue line and read off X of mineral extract

Results:

Remove plagioclase, olivine, pyroxene and Fe-Ti oxide

Oxide	Wt%	Cation Norm	
SiO_2	46.5	ab	18.3
TiO_2	1.4	an	30.1
Al_2O_3	14.2	di	23.2
Fe_2O_3*	11.5	hy	4.7
MgO	10.8	ol	19.3
CaO	11.5	mt	1.7
Na_2O	2.1	il	2.7
K_2O	0		
Total	98.1		100

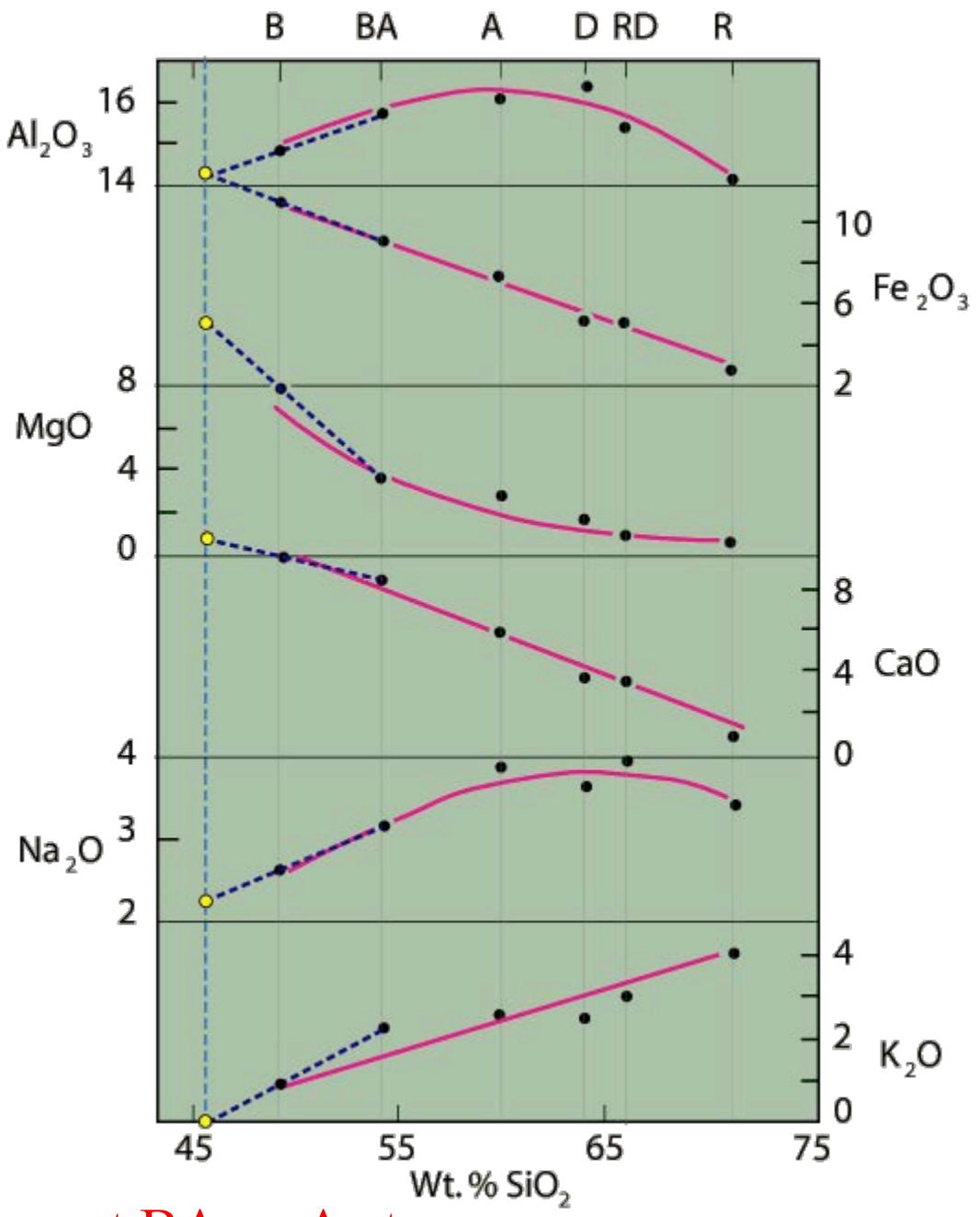

Then repeat for each increment BA → A etc.

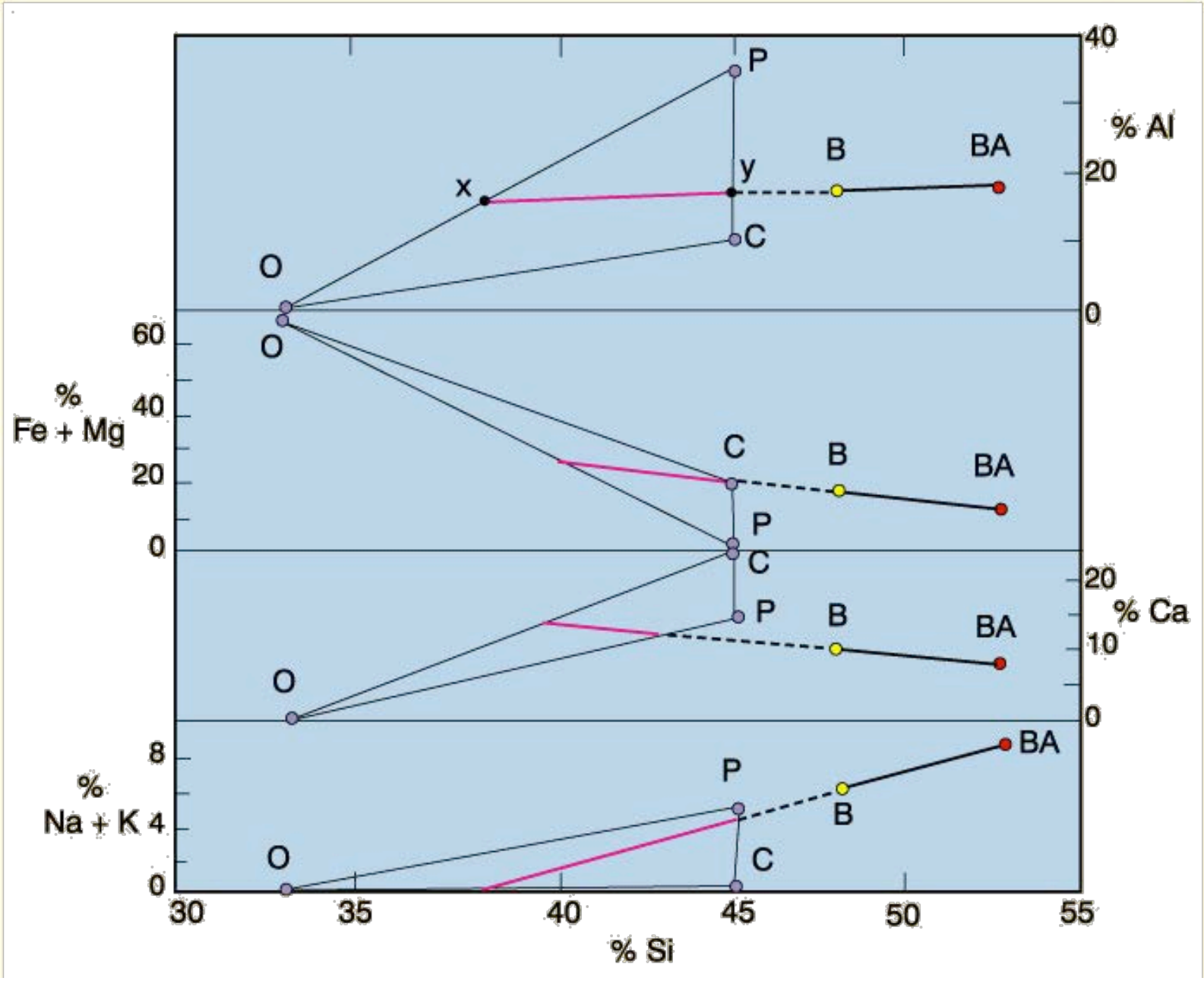

Figure 8.8. Variation diagram on a cation basis for the fractional crystallization of olivine, augite, and plagioclase to form BA from B (Table 8-6). From Ragland (1989). Basic Analytical Petrology, Oxford Univ. Press.

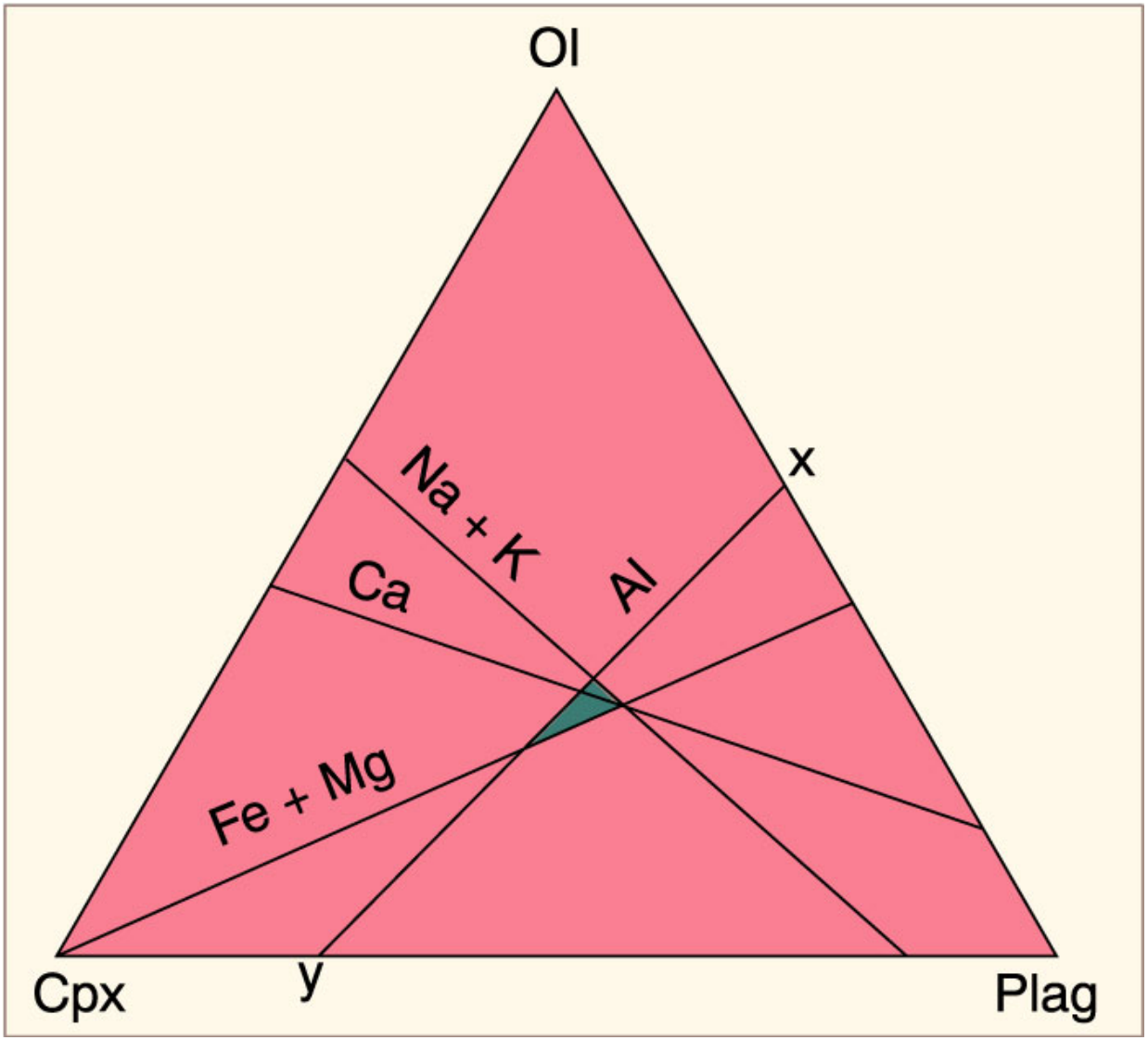

Figure 8.9. Equilateral triangle showing the solution to the bulk mineral extract (shaded area) best fitting the criteria for the variation diagrams in Figure 8-8. From Ragland (1989). Basic Analytical Petrology, Oxford Univ. Press.

Magma Series

Can chemistry be used to distinguish ***families*** of magma types?

Early on it was recognized that some chemical parameters were very useful in regard to distinguishing magmatic groups

- Total Alkalis ($Na_2O + K_2O$)
- Silica (SiO_2) and silica saturation
- Alumina (Al_2O_3)

Alkali vs. Silica diagram for Hawaiian volcanics:

Seems to be two distinct groupings: ***alkaline*** and ***subalkaline***

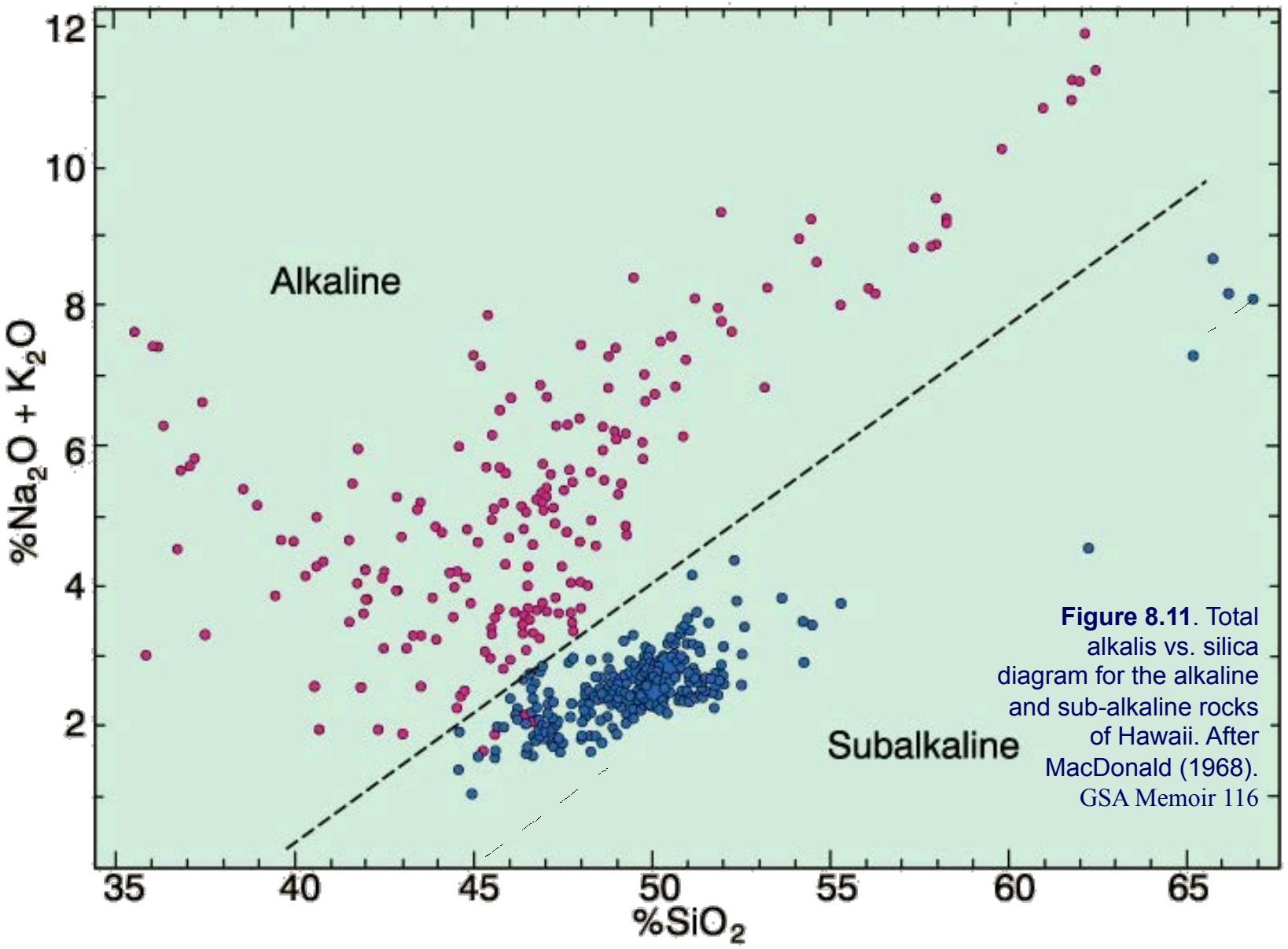

Figure 8.11. Total alkalis vs. silica diagram for the alkaline and sub-alkaline rocks of Hawaii. After MacDonald (1968). GSA Memoir 116

The Basalt Tetrahedron and the Ne-Ol-Q base

Alkaline and subalkaline fields are again distinct

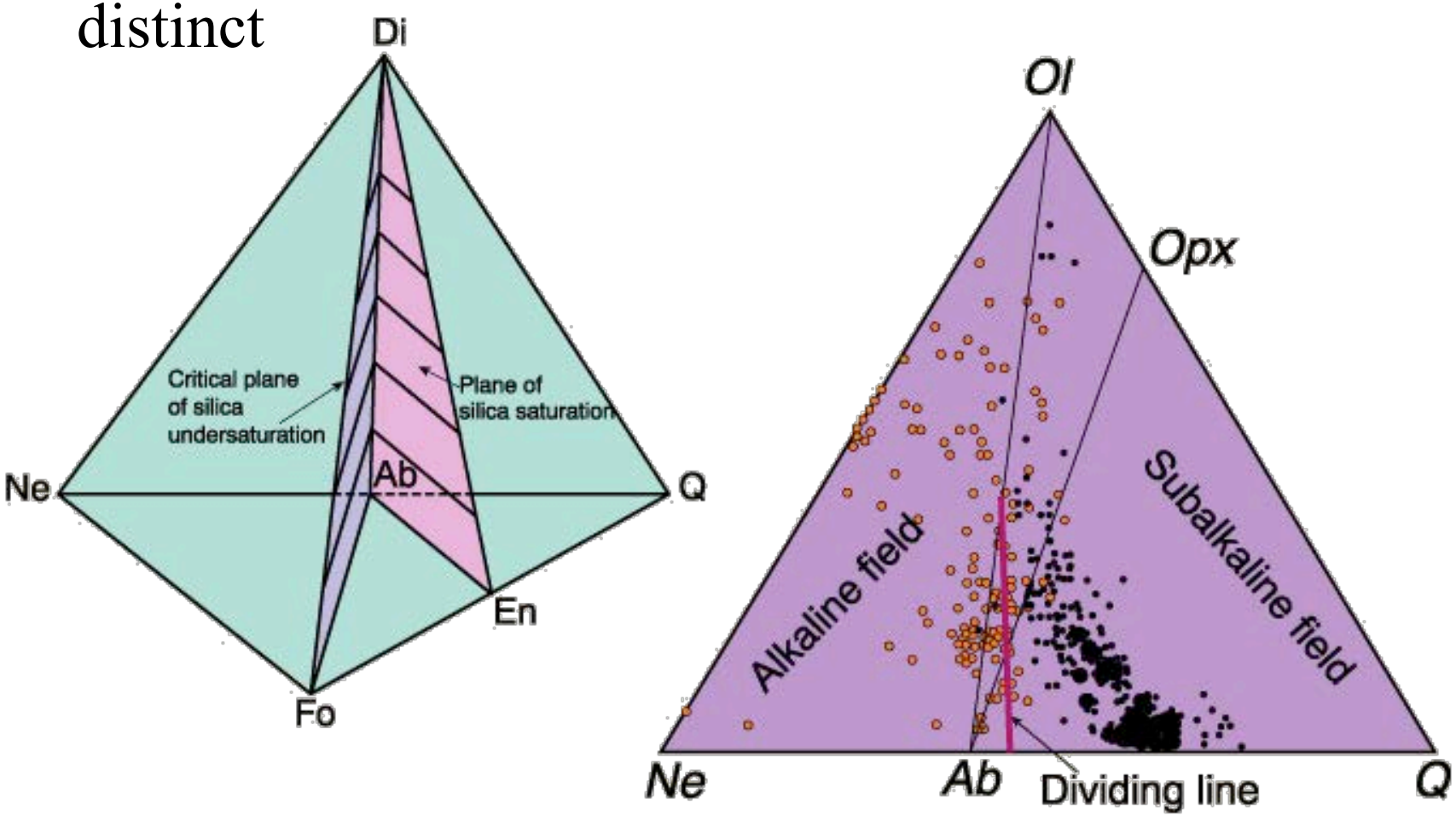

Figure 8.12. Left: the basalt tetrahedron (after Yoder and Tilley, 1962). J. Pet., 3, 342-532. Right: the base of the basalt tetrahedron using cation normative minerals, with the compositions of subalkaline rocks (black) and alkaline rocks (gray) from Figure 8-11, projected from Cpx. After Irvine and Baragar (1971). Can. J. Earth Sci., 8, 523-548.

Thermal divide separates the silica-saturated (subalkaline) from the silica-undersaturated (alkaline) fields at low pressure

Cannot cross this divide by FX, so can't derive one series from the other (at least via low-P FX)

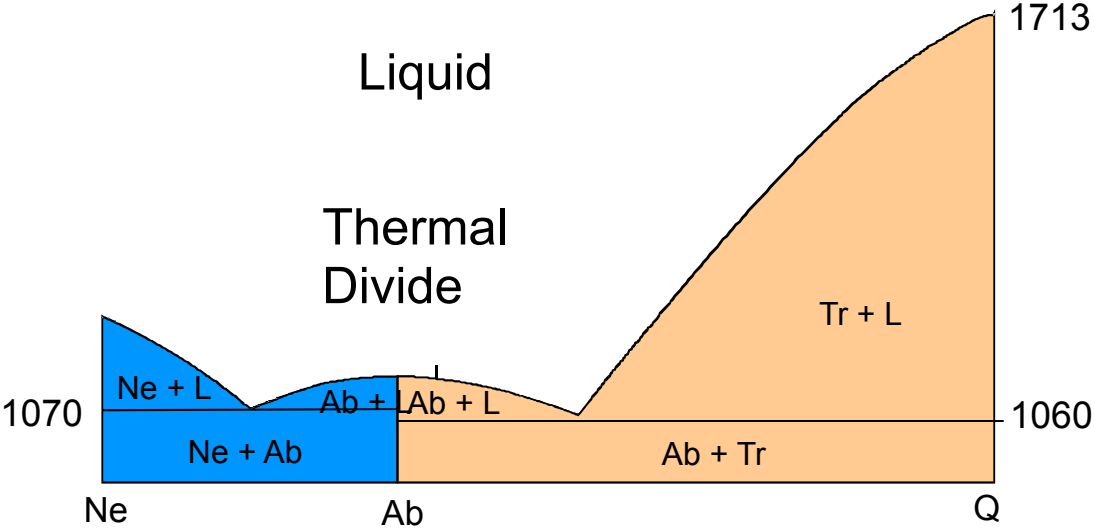

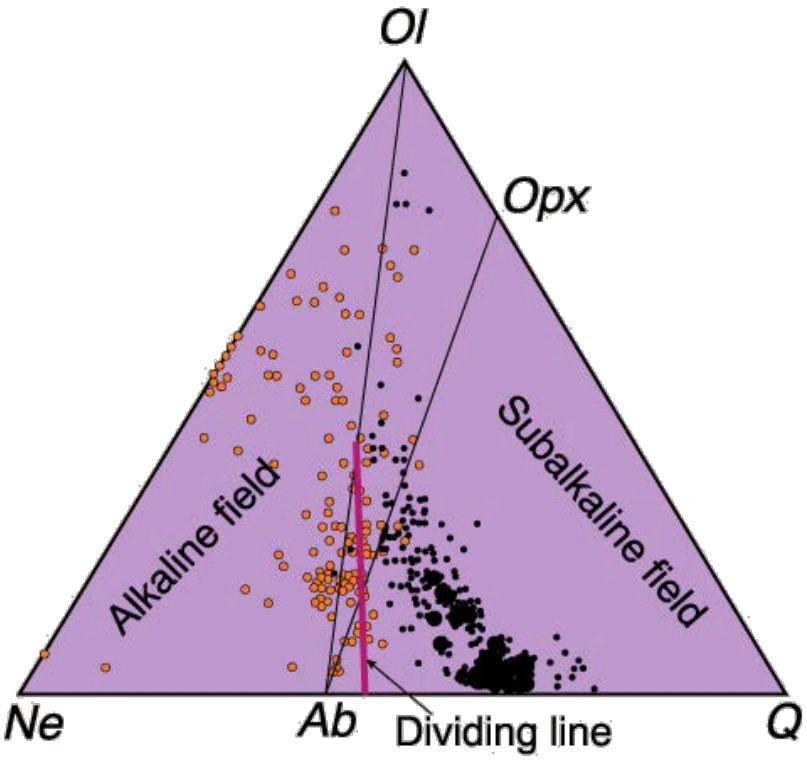

AFM diagram: can further subdivide the subalkaline magma series into a ***tholeiitic*** and a *calc-alkaline* series

Figure 8.14. AFM diagram showing the distinction between selected tholeiitic rocks from Iceland, the Mid-Atlantic Ridge, the Columbia River Basalts, and Hawaii (solid circles) plus the calc-alkaline rocks of the Cascade volcanics (open circles). From Irving and Baragar (1971). After Irvine and Baragar (1971). Can. J. Earth Sci., 8, 523-548.

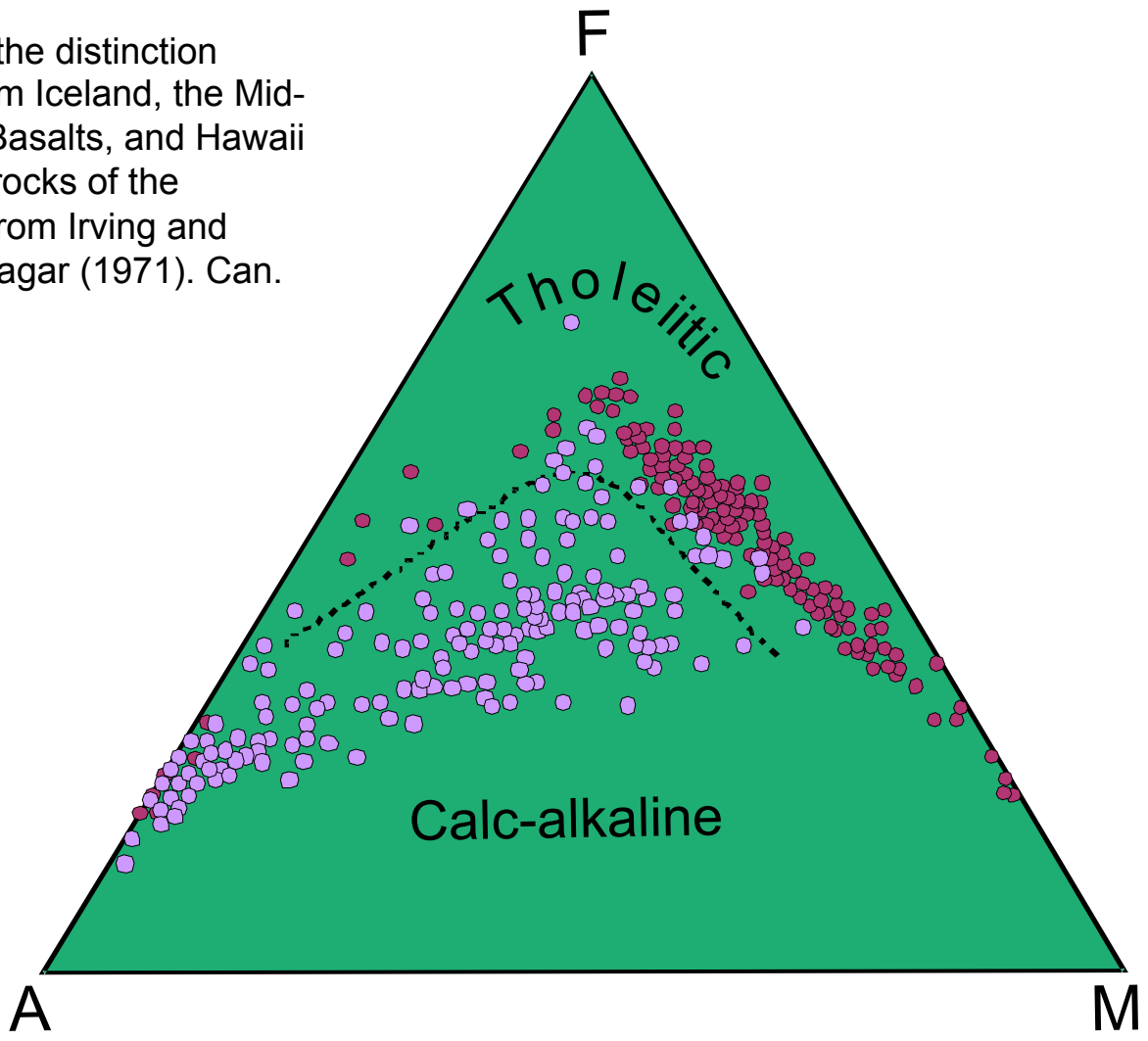

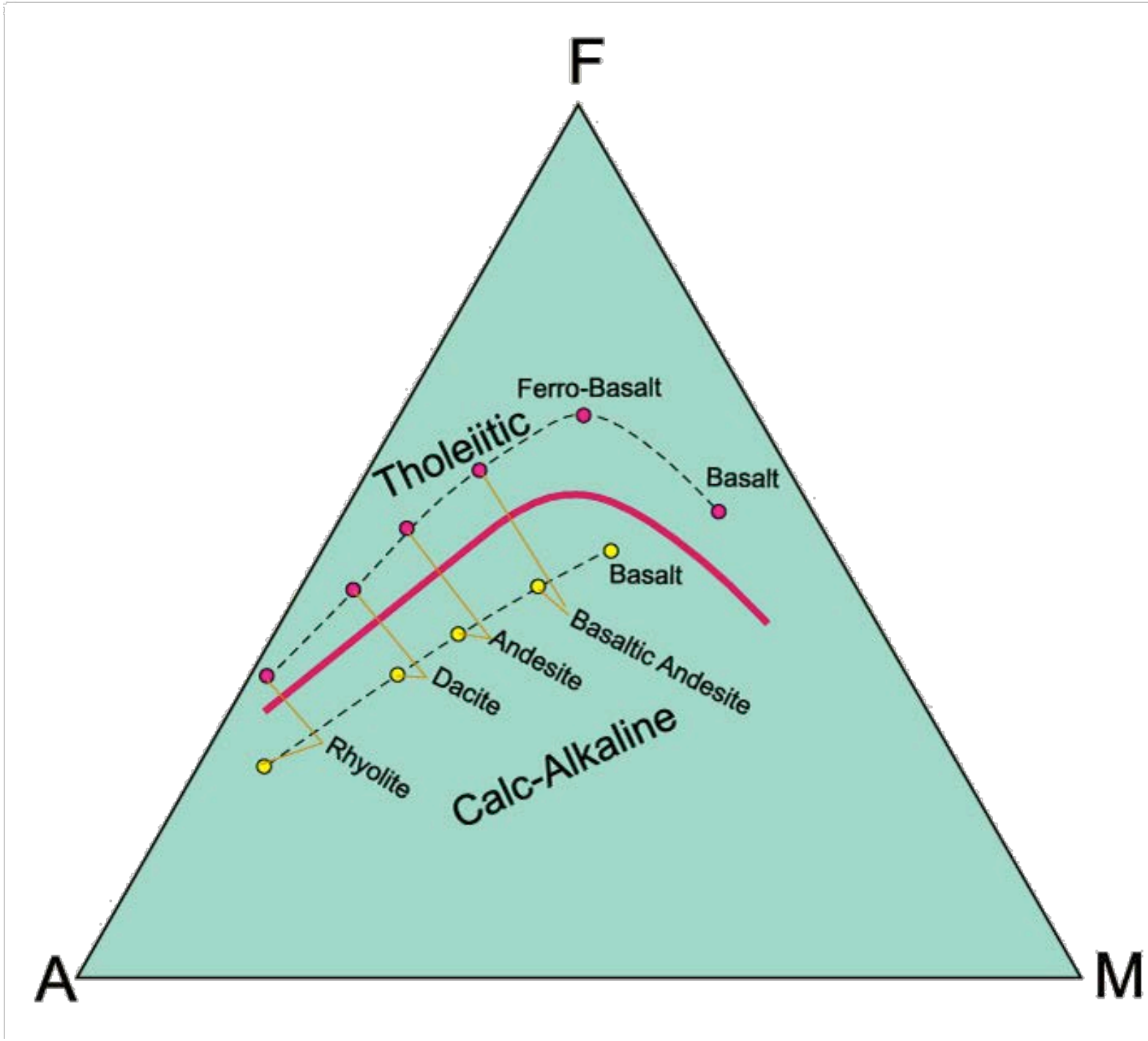
F
A
M
Ferro-Basalt
Tholeiitic
Basalt
Basalt
Basaltic Andesite
Andesite
Dacite
Rhyolite
Calc-Alkaline

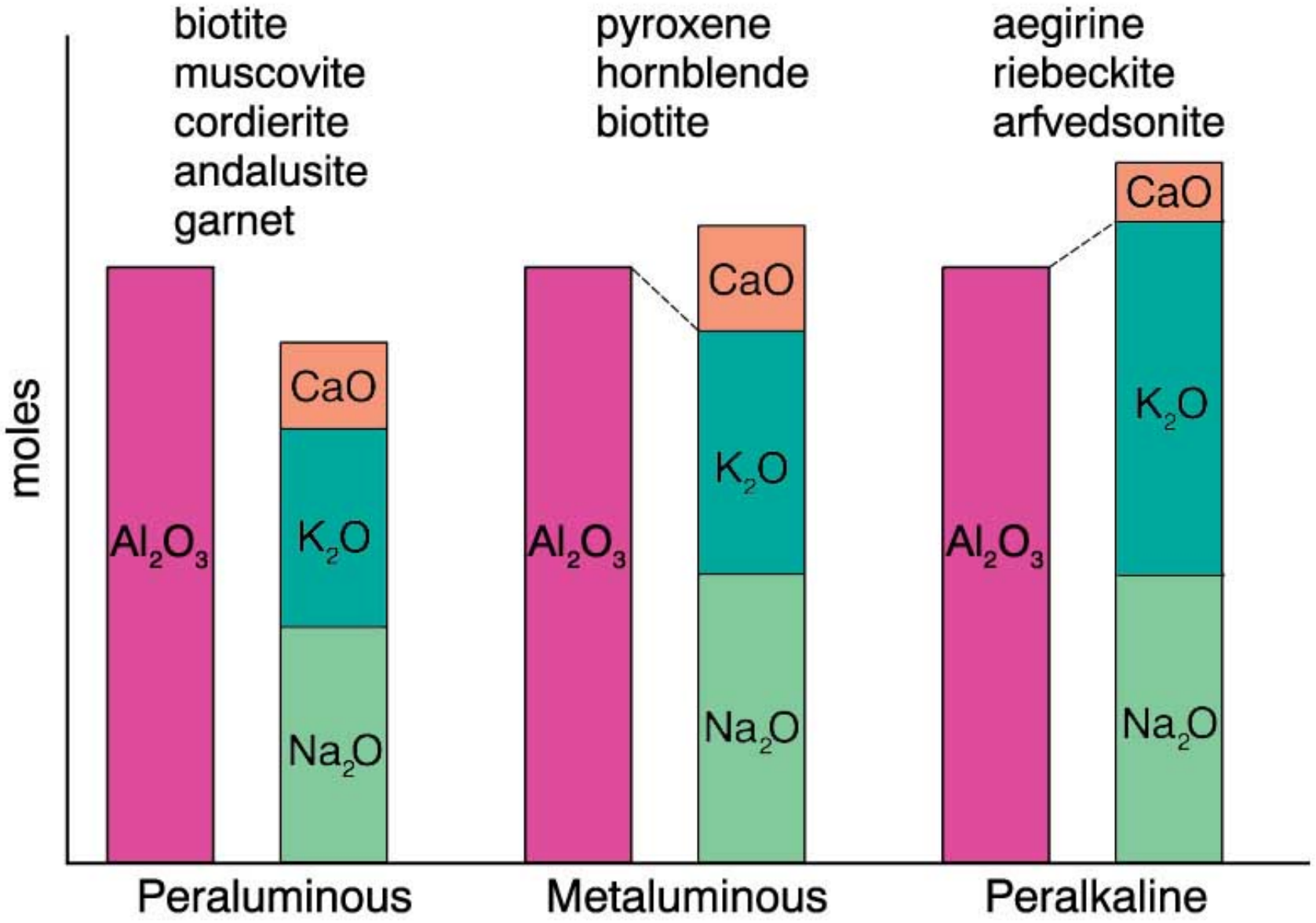

Figure 18.2. Alumina saturation classes based on the *molar* proportions of $Al_2O_3/(CaO+Na_2O+K_2O)$ ("A/CNK") after Shand (1927). Common non-quartzo-feldspathic minerals for each type are included. After Clarke (1992). Granitoid Rocks. Chapman Hall.

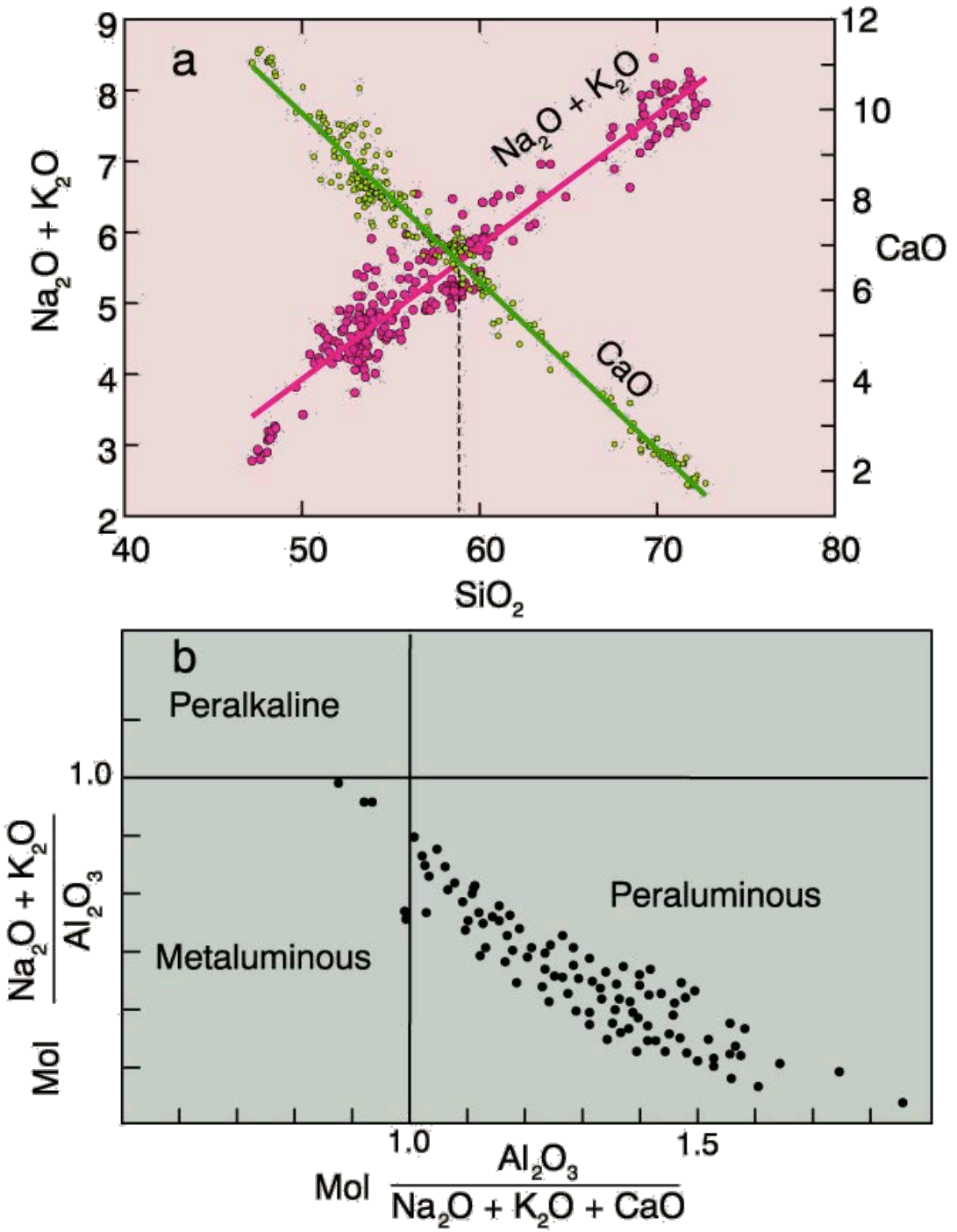

Figure 8.10

a. Plot of CaO (green) and (Na_2O + K_2O) (red) vs. SiO_2 for the Crater Lake data. Peacock (1931) used the value of SiO_2 at which the two curves crossed as his "alkali-lime index" (dashed line).

b. Alumina saturation indices (Shand, 1927) with analyses of the peraluminous granitic rocks from the Achala Batholith, Argentina (Lira and Kirschbaum, 1990). In S. M. Kay and C. W. Rapela (eds.), Plutonism from Antarctica to Alaska. Geol. Soc. Amer. Special Paper, 241. pp. 67-76.

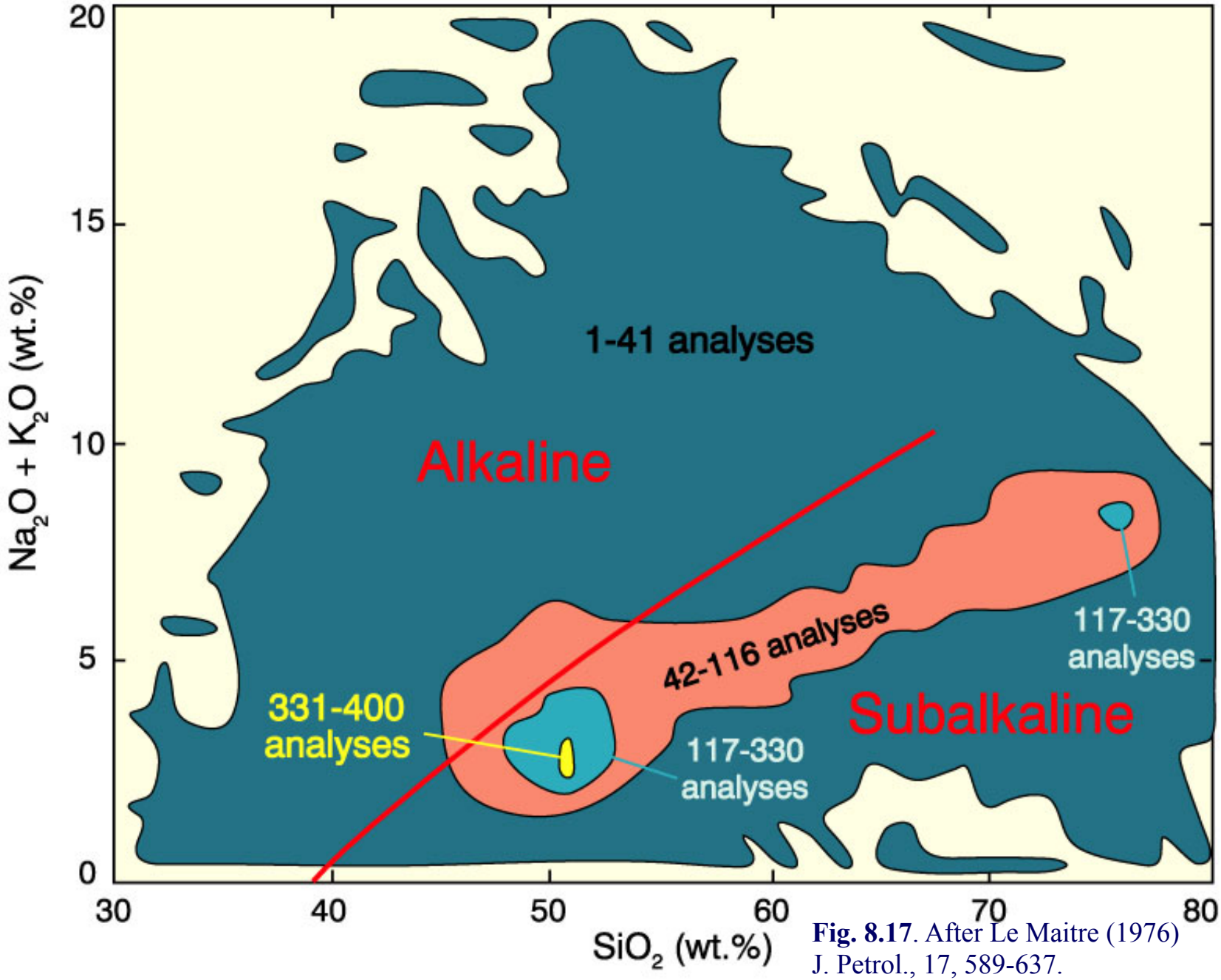

Fig. 8.17. After Le Maitre (1976) J. Petrol., 17, 589-637.

A world-wide survey suggests that there may be some important differences between the three series

Characteristic Series	Plate Margin		Within Plate	
	Convergent	Divergent	Oceanic	Continental
Alkaline	yes		yes	yes
Tholeiitic	yes	yes	yes	yes
Calc-alkaline	yes			

After Wilson (1989). Igneous Petrogenesis. Unwin Hyman - Kluwer

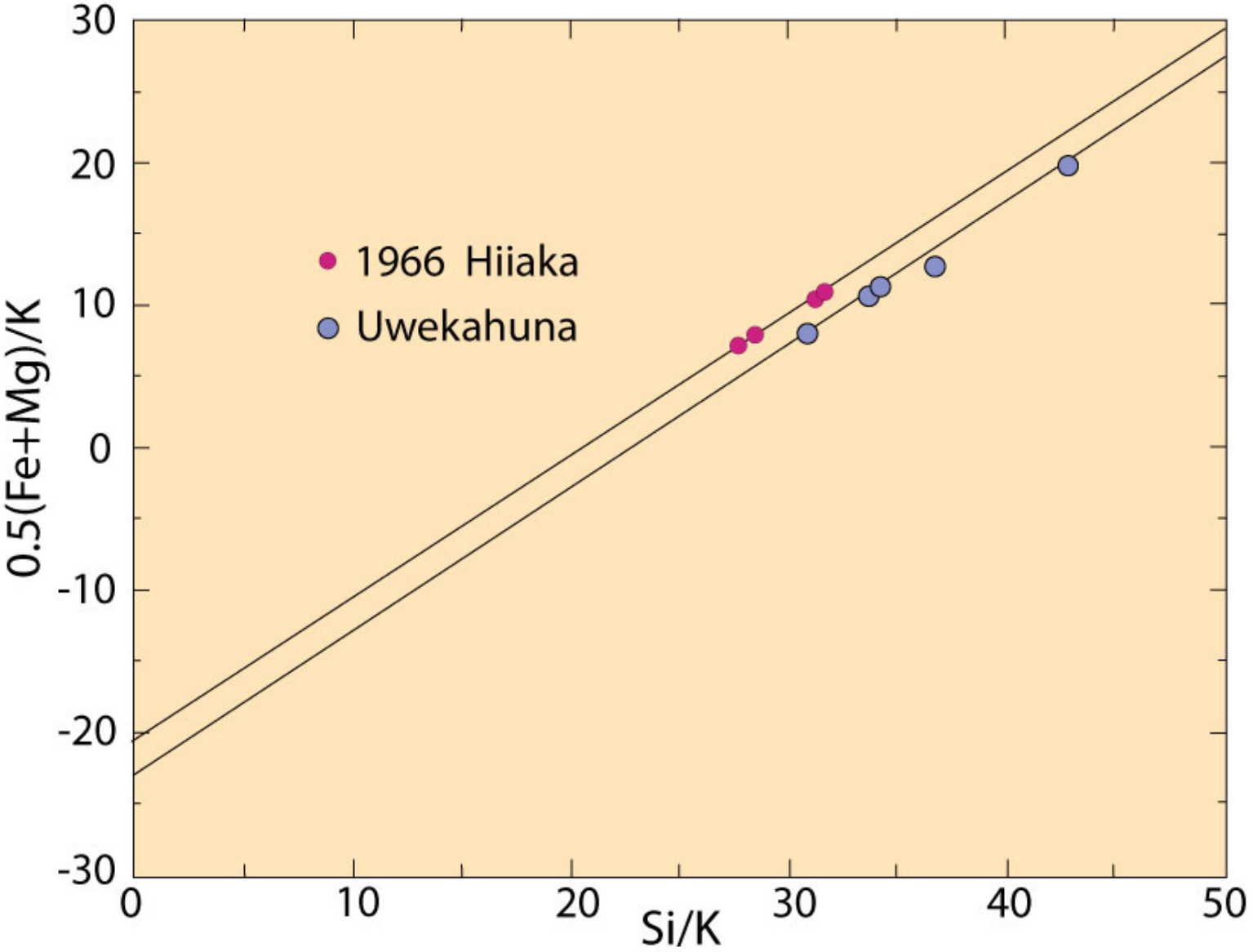

Figure 8.4. Pearce element diagram of 0.5(Fe + Mg)/K vs. Si/K for two Hawaiian picritic magma suites. From Nicholls and Russell (1990).

Figure 8.5. Pearce element diagrams for basalts (dark circles) and picrites (light circles) erupted from Kilauea, Hawaii, between November, 1967 and August, 1968. After Nicholls (1990).

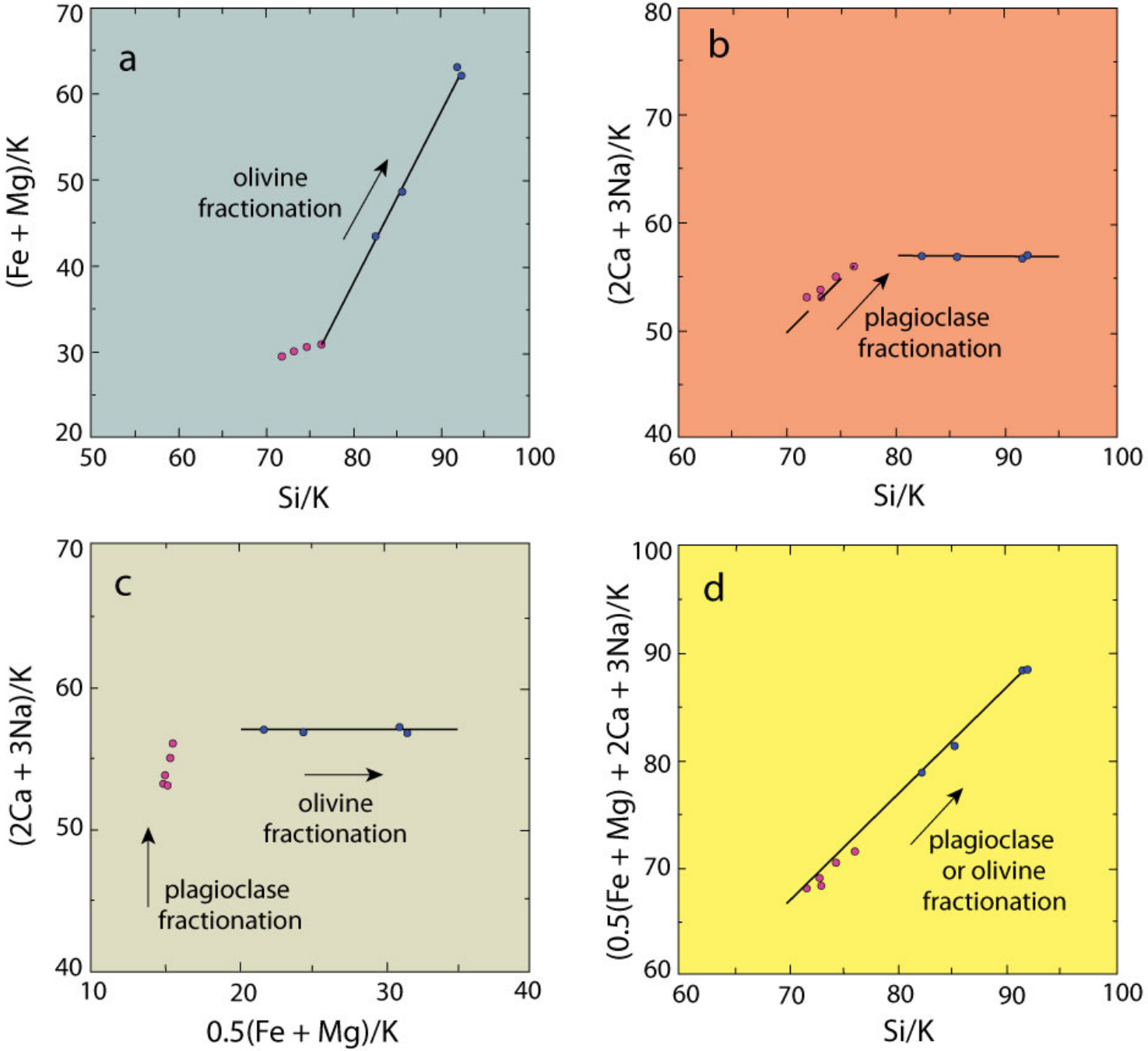

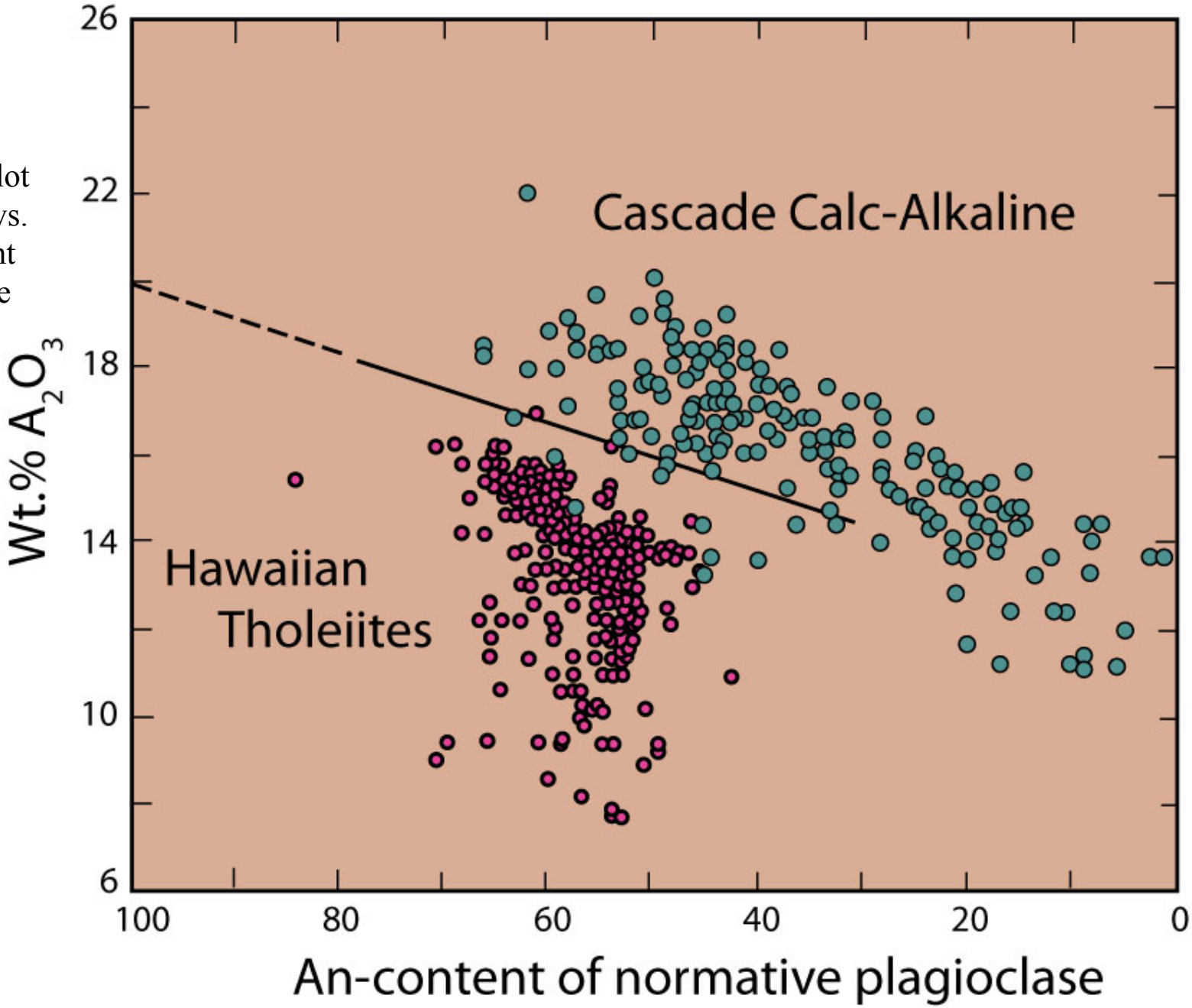

Figure 8.15. Plot of wt.% Al_2O_3 vs. anorthite content of the normative plagioclase, showing the distinction between the tholeiitic and calc-alkaline series. From Irvine and Baragar (1971).

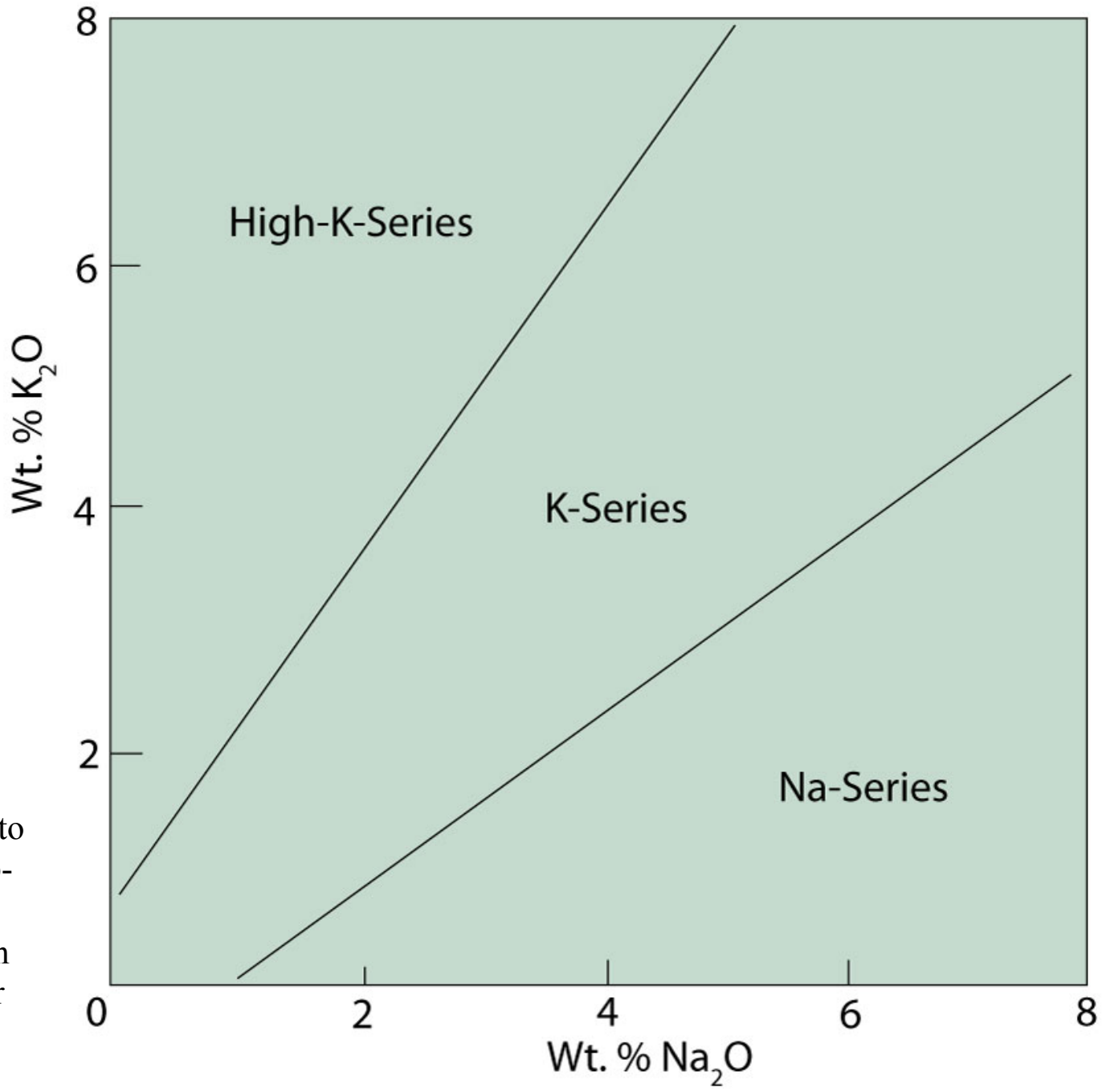

Figure 8.16.
Wt.% K_2O vs. Na_2O diagram subdividing the alkaline magma series into High-K-, K-, and Na-sub-series. After Middlemost (1975). Copyright © with permission from Elsevier Science.